Design and Evaluation of an Inductive Powering Unit for Implantable Medical Devices Using GPU Computing

Arseny A. Danilov, Eduard A. Mindubaev[*], and Sergey V. Selishchev

Abstract—Nowadays inductive powering has become a widely spread technique in existing and emerging implanted medical devices (IMD). The geometry of coils couple plays a key role in the design, optimization and evaluation of a biomedical inductive powering unit (IPU). We have proposed a relatively fast method for an execution of these procedures, which is based on a mutual induction calculation using GPU parallel computing. Generally, our approach is to calculate mutual inductance as a function of uncontrolled (axial distance, lateral distance, inclination) and controlled (coils radii, turns numbers, distance between turns) geometric parameters of a coil couple. Calculated geometric functions in its turn are used in the design and optimization procedure to evaluate an IPU performance (e.g., load power). Achieved time gain of the GPU calculations in comparison with the host CPU computing is up to 80 for sequential summation and up to 8 for parallel computing. Also, it is shown that precision of our method is comparable to the precision of existing electromagnetic field solvers, and at the same time, computation time is substantially less (time gain is about 7 ... 8 for 2D case and about 100 and higher for 3D case). Additionally, we have verified our method experimentally and shown that results of the calculations are accurate enough to predict real IPU performance. Finally, we have given an example of an IPU design optimization using geometric functions calculated with the help of the proposed method.

1. INTRODUCTION

Transcutaneous energy transfer via an inductive link is an emerging technology in modern biomedical engineering [1–3] and becomes a common powering method in cochlear implants and spinal cord stimulators [4–6], and is proposed for a wide variety of implanted medical devices (IMD), from visual prostheses [7, 8] to smart orthopedic implants [9, 10]. Wireless powering of mechanical circulatory support systems is of special interest [11–16].

Energy supply of an IMD is a complex task in itself. The major issues here are size limitation, severe operating condition and strict safety considerations, which include reliability, biocompatibility, stability and predictability [17, 18]. Adding a wireless link makes the problem even more difficult. Consequently, although history of a transcutaneous energy transfer began simultaneously with history of an IMD [19, 20], there are still problems to be solved, and the design of inductive powering unit (IPU) still represents a serious challenge.

Generally speaking, powering of an IMD is a device-specific task [1, 21]. Nevertheless, one can distinguish several almost universal problems and solutions. Energy transfer efficiency, energy transfer stability and thermal safety are primary concerns in any case [13]. All these problems are associated with fundamental difficulty of an implant inductive powering, namely, inevitable coils displacements and misalignments [1, 22–24]. On the other hand, we can find typical geometry (coils of almost equal size, distance between coils is lesser than coils size, linear dimensions of the order of 0.1 ... 1 cm) and operating frequency in close range (namely, 0.1 ... 10 MHz) in most design examples. Generally

speaking, most IPUs for IMDs operate in near-field region [25]. Thus, it is possible to derive common design principles and propose common design tools for biomedical IPU.

It can be argued that inductive link geometry constitutes a key factor in IPU development [26–28]. This geometry can be described in terms of controlled and uncontrolled parameters. Controlled parameters include coils radii, wire radii, the distance between turns and turns number. Uncontrolled parameters include linear and angular characteristics of a coils mutual position (lateral distance, axial distance, inclination). All these parameters can greatly affect IPU performance. For example, it is shown that inductive link efficiency can be significantly improved even by adjustment of the distance between the turns [26]. Moreover, the character of geometry influence may reverse depending on circumstances. In particular, changes in a coils mutual position can lead to underload as well as overload of a system [23, 28]. Thus, full information about the interrelation between all geometric parameters and IPU performance metrics is essential to finding new ways for optimization and greatly enhances design procedure potential.

The centerpiece of such a procedure is calculation of a mutual inductance as a function of geometric parameters. There are several formulas which can be used, from well-known Neumann's one to the contemporary works of Babic and Conway [29–37]. Another way of mutual inductance calculation is the use of existing electromagnetic field solvers (EFS). But usually it is a time-consuming procedure, and that is especially important in our case when significant data amount should be calculated and processed. Moreover, it is often difficult and sometimes even impossible to obtain mutual inductance as a function of geometry with available products. Thus, field solvers are used commonly for the verification of design features and rarely for a design itself [21, 27].

The main goal of the work is to present relatively fast and sufficiently accurate tool for geometric evaluation of an IPU performance, which can be used in design and optimization procedure. In order to achieve this, we propose a method for parallel computation of a coil couple mutual inductance as a function of geometric parameters. It is described in detail in Section 1 as well as mathematics for calculation of IPU performance metrics in dependence of a mutual inductance. There is always tradeoff between speed and accuracy of calculations, and we address this problem in Section 2. It is found that evaluation of an inductive link in specific geometry with our method can be performed in a reasonably short time (of the orders of hours or days). In order to analyze the accuracy we compare results of our calculations with ones obtained with the existing field solvers and with experimental data. Results of comparison suggest that our method is accurate enough to predict performance characteristics of a real inductive link. Finally, in Section 3 we give some ideas about how our calculations can be used for design and optimization of an IPU. Example of an inductive link design is presented to illustrate possible approach to application of our method.

2. IPU PERFORMANCE MODELING

Mutual inductance is the main characteristic for analysis of the inductive link geometry. It can be defined as ratio between current in primary winding and electromotive force in secondary winding induced by this current. At the same time, mutual inductance can be derived from purely geometric considerations. The simplest (and thus less computationally expensive) way to extract mutual inductance for a pair of infinitely thin and arbitrary oriented filaments is so-called Neumann's formula [38]:

$$M_F = \frac{\mu_0}{4\pi} \oint_{l_t} \oint_{l_r} \frac{d\overrightarrow{l_t}\, d\overrightarrow{l_r}}{r_{tr}}, \tag{1}$$

here μ_0 is magnetic permeability of a vacuum; R_t and R_r are transmitting and receiving coil turns radii; φ is the angle of inclination between the two circuit elements $d\overrightarrow{l_t}$ and $d\overrightarrow{l_r}$; r_{tr} is the distance between this elements.

Infinitely thin filaments approximation means that current distribution across the wire is neglected. It means that the presented method for calculation of mutual inductance does not account for wire thickness influence on the mutual inductance in the same way electromagnetic solvers do. However, this assumption is justified, and it is fair to use Equation (1), if geometric sizes of the coils (i.e., coils radii) and distance between the coils are much greater than wire cross-section radii (that point is verified by

measurements in Section 3.3 of the article) [39]. It is also worth mentioning that effect of the tissues on the mutual inductance can be described using the Neumann's formula by multiplying Equation (1) by relative magnetic permeability of surrounding medium. However, biological tissues can be considered with high precision as diamagnetics ($\mu = \mu_0$) [40, 41]. Therefore, the aforementioned effect can be neglected. Moreover, constant current distribution along the wire is assumed. Finally, air-cored coils are considered as a common choice in biomedical applications, and thus relative magnetic permeability of the medium is taken as 1. Also, possible effect of ferrite substrate or shielding plates is not taken into account. If these components are part of the proposed IPU design, their effect can be easily incorporated in the calculation by adding a ΔM term in the same manner as in [42].
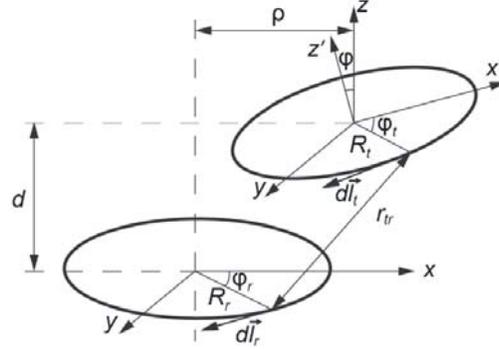
Figure 1. Geometry of a coil couple in an IPU design. Uncontrolled geometric parameters (lateral distance d, axial distance ρ, inclination φ) greatly affect IPU performance and thus geometric evaluation is essential for a proper IPU design.

For a pair of filaments positioned as shown in Fig. 1 (with axial distance d and lateral misalignment ρ) it can be written:

$$M_F = \frac{\mu_0}{4\pi} R_t R_r \int\limits_0^{2\pi} \int\limits_0^{2\pi} \frac{(\cos\varphi \cos\varphi_t \cos\varphi_r + \sin\varphi_t \sin\varphi_r)\, d\varphi_r d\varphi_t}{r_{tr}}, \tag{2}$$

where r_{tr} can be calculated as follows

$$\begin{cases} r_{tr} = \sqrt{(x_t - x_r)^2 + (y_t - y_r)^2 + (z_t - z_r)^2} \\ x_t - x_r = \rho + R_t \cos\varphi_t \cos\varphi - R_r \cos\varphi_r \\ y_t - y_r = R_t \sin\varphi_t - R_r \sin\varphi_r \\ z_t - z_r = d + R_t \cos\varphi_t \sin\varphi \end{cases} \tag{3}$$

In the case of biomedical applications, inclination angle is usually relatively small (not more than 15 ... 20 degrees, see, for example [38]). It is so because the distance between the coils is less than the coils radii, and biological tissue between the coils prevents large angular misalignment. Consequently, we can assume that $\cos\varphi \approx 1$, and modify Equation (2):

$$M_F \approx \frac{\mu_0}{4\pi} R_t R_r \int\limits_0^{2\pi} \int\limits_0^{2\pi} \frac{\cos(\varphi_t - \varphi_r)\, d\varphi_r d\varphi_t}{r_{tr}}. \tag{4}$$

It can be seen that the assumption greatly reduces computational time, because it eliminates four trigonometric functions as well as three multiplication operations. The effect of this assumption on the computation accuracy and speed of the calculations will be addressed extensively in Section 3.1.

In general case, when d, ρ, $\varphi \neq 0$, a closed-form expression of a Neumann's formula (1) cannot be derived. At the same time, that case is specific for transcutaneous energy transfer. Thus, one needs to obtain approximate expression (see, for example [38]) or use numerical integration for calculation of mutual inductance. In the latter case, it can be written using rectangle method:

$$M_F = \frac{\mu_0 R_t R_r}{4\pi} \sum_{n=1}^{N} \sum_{k=1}^{K} \frac{\cos(\varphi_k - \varphi_n)\, \Delta\varphi_t \Delta\varphi_r}{r_{kn}} = \frac{\mu_0 \pi R_t R_r}{NK} \sum_{n=1}^{N} \sum_{k=1}^{K} \frac{\cos(\varphi_k - \varphi_n)}{r_{kn}}, \tag{5}$$

here $\Delta\varphi_t = 2\pi/N$, $\Delta\varphi_r = 2\pi/K$, $\varphi_k = 2\pi k/K$, $\varphi_n = 2\pi n/N$, N is the number of turn elements in transmitter coil and K the number of turn elements in receiver coil.

Expression for mutual inductance of a couple of coils with turns number N_{wt} and N_{wr} is written as follows:

$$M_C = \sum_{i=1}^{N_{wt}} \sum_{j=1}^{N_{wr}} M_{F_{ij}} = \frac{\mu_0}{4\pi} \sum_{i=1}^{N_{wt}} \sum_{j=1}^{N_{wr}} R_{t_i} R_{r_j} \int_0^{2\pi} \int_0^{2\pi} \frac{\cos\left(\varphi_{r_j} - \varphi_{t_i}\right) d\varphi_{r_j} d\varphi_{t_i}}{r_{t_i r_j}}. \tag{6}$$

here i and j are the turns indices.

Each turn of a coil with multiple turns can be represented as a number of closed loops parallel to each other. Mutual inductance between the transmitting and receiving coils can be treated as double sum of mutual inductances between the discrete loops of the coils [39]. Expression (6) is generalized in terms of turns radii and can be applied to spiral coils as well as to cylindrical (in the last case, turns radii are equal to each other and thus can be set before the double sum). It should be noted that Eq. (3) should be modified for calculation of $r_{t_i r_j}$. Namely, distance between the turns should be taken into account in accordance with the coils form-factor. Wire thickness is also accounted only as a parameter which affects distance between the turns to initialize relative distance between the filaments.

Substituting Eq. (5) in Eq. (6), one can obtain the following expression:

$$M_C = \mu_0 \pi \sum_{i=1}^{N_{wt}} \sum_{j=1}^{N_{wr}} \frac{R_{t_i} R_{r_j}}{N_i K_j} \sum_{n_i=1}^{N_i} \sum_{k_j=1}^{K_j} \frac{\cos\left(\varphi_{k_j} - \varphi_{n_i}\right)}{r_{k_j n_i}}. \tag{7}$$

If turns in both coils are divided into an equal number of elements, expression (5) can be written as follows:

$$M_C = \frac{\mu_0 \pi}{NK} \sum_{i=1}^{N_{wt}} \sum_{j=1}^{N_{wr}} R_{t_i} R_{r_j} \sum_{n_i=1}^{N} \sum_{k_j=1}^{K} \frac{\cos\left(\varphi_{k_j} - \varphi_{n_i}\right)}{r_{k_j n_i}}. \tag{8}$$

Operation under constantly changing geometric conditions is a feature of an IMD inductive powering unit. Therefore, proper geometric evaluation of an IPU performance requires calculation of a set of mutual inductance values for the given range of uncontrolled geometric parameters (namely, d, ρ, φ). Furthermore, during an IPU design process, this evaluation must be performed for a number of controlled parameters as well. Thus, if there are N_P uncontrolled geometric parameters for the given range and N_D versions of the IPU design, $N_D N_p N_{wt} N_{wr} N K$ calculations of a basic function $\cos\left(\varphi_{k_j} - \varphi_{n_i}\right)/r_{k_j n_i}$ are required for complete evaluation of the IPU operation. This number can reach values of $10^7 \ldots 10^{12}$ depending on necessary problem discretization. Such a problem can be effectively dealt with by parallel computing.

Today one of the most popular parallel computing techniques is GPU computing [43, 44]. In this work, NVIDIA Tesla C2075 graphical processor and MATLAB coding were used. There are several possible ways to solve the problem of an IPU geometric evaluation with these tools. Method which is both flexible and relatively simple was chosen, and thus it can be implemented by designers without advanced knowledge in area of parallel computing.

We decided to calculate the mutual inductance for fixed values of controlled parameters and for one set of a single uncontrolled parameter in one GPU run. In this case, the number of available parallel threads N_T (that said, 1024) is much larger than the number of geometric parameter values N_P (that said, 10 ... 20) which is sufficient for IPU performance analysis. Thus, main feature of a proposed procedure is a two-way parallelism. First, we split calculation procedure into N_P calculation blocks. Each block corresponds to one point in a geometric parameter set. Second, we split low order sum in Equation (8) into a number of sub-sums in accordance with a number of available threads in calculation block. Detailed procedure is described below:

1. Determine constant values. In our method, all controlled and uncontrolled geometric parameters geometric parameters are constant, except one uncontrolled parameter (e.g., d, ρ or φ).

2. Define a main index $g = [1, 2, \ldots, N_T]$ in GPU array. In general case, parallel threads in GPU computing are independent from each other, and thus for every GPU run all necessary data must

be translated in GPU or calculated inside a thread body. Main index must be defined to calculate geometric parameter value and index brackets for low-order sub-sum inside every parallel thread.

3. Choose the number of points in a set of geometric parameter values N_P so that $N_T \bmod N_P = 0$. In other words, N_P should be a divisor of N_T. Then establish a set of geometric parameter values so that $P = [P_1, \ldots, P_q, \ldots, P_{N_P}]$.

4. Calculate the number of parallel threads for every calculation block associated with one point in geometric parameter set N_{ST} as follows:

$$N_{ST} = [N_T/N_P], \tag{9}$$

here $[\bullet/\bullet]$ is an integer division.

5. Choose the number of turn elements for the receiver coil (and the number of operations for low-level sum in Eq. (8)) K so that $K \bmod N_{ST} = 0$. In other words, N_{ST} should be a divisor of K. Analogously, choose the number of turn elements for the transmitter coil N.

6. Transfer all the data mentioned above to a GPU.

7. Calculate the value of an uncontrolled geometric parameter corresponding to a gth thread as

$$P_g = P_{\min} + \left[\frac{(g-1)}{N_{ST}} \right] \frac{(P_{\max} - P_{\min})}{N_P - 1}, \tag{10}$$

here $P_{\min}$ and $P_{\max}$ are minimal and maximal values of a geometric parameter respectively. Note that value of the geometric parameter stays the same inside every block of parallel threads associated with one point in the geometric parameter set. The index of the point is defined by $[\frac{(g-1)}{N_{ST}}]$ term.

8. Split every low level sum into N_{ST} sub-sums and calculate intermediate values inside gth thread using the following expression:

$$M'_g = \sum_{i=1}^{N_{wt}} \sum_{j=1}^{N_{wr}} R_{t_i} R_{r_j} \sum_{n_i=1}^{N} \sum_{k_j=K'}^{K''} \frac{\cos\left(\varphi_{k_j} - \varphi_{n_i}\right)}{r_{k_j n_i}}, \tag{11}$$

here $K'' = (g - N_{ST}[(g-1)/N_{ST}])[K/N_{ST}]$, $K' = K'' - [K/N_{ST}] + 1$, $t = 1 \ldots N_{ST}$. Note that values of geometric parameters obtained via Eq. (10) are included implicitly in $r_{k_j n_i}$ term according to Eq. (3).

9. Gather values M'_g from the GPU and transfer them to the global memory array $M' = [M'_1, \ldots, M'_g, \ldots, M'_{N_T}]$.

10. Calculate values of the mutual inductance as a function of the geometric parameter by sequential summation of N_{ST}-elements sequences in M' for every geometric point

$$M_C\left(P_q\right) = \frac{\mu_0 \pi}{NK} \sum_{t=qN_{ST}+1}^{(q+1)N_{ST}} M'_t, \tag{12}$$

here $q = [\frac{(g-1)}{N_{ST}}]$ is the sequential number of the geometric points.

Steps 7, 8, 9 and 10 are depicted in Fig. 2 for better clarification of the procedure.

Described procedure returns the mutual inductance as a function of the single geometric parameter. It can be repeated for another geometric parameter or another set of controlled parameter in order to perform more detailed geometric evaluation or for optimization of the IPU design as will be shown later.

3. PERFORMANCE MEASUREMENT

The main goal of our work, as mentioned above, is to speed up calculation of the mutual inductance with acceptable accuracy. We studied the performance of the proposed method in terms of computational cost, achieved time-gain and accuracy using both numerical calculation and experimental verification. Results of the study are summarized below.
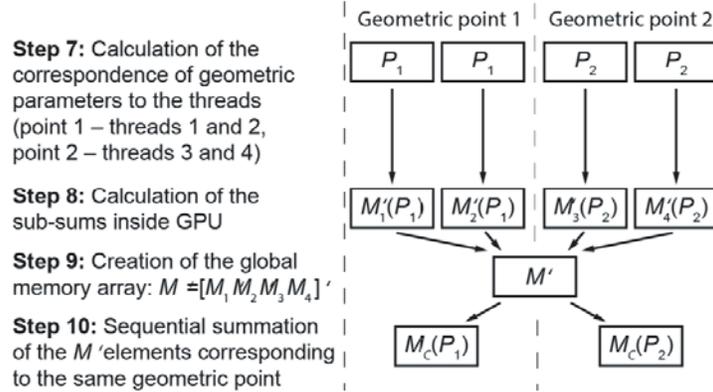
Figure 2. Demonstration of the steps from 7th to 10th of the proposed method. This example shows the parallelization for four threads and two geometric points.

3.1. Method Computation Time as Compared to the CPU Computing

Usually IPU design for biomedical implants incorporates a couple of coils with $10 \ldots 20$ turns. It was found that with the proposed method and above-mentioned hardware it takes about $10 \ldots 80$ seconds to calculate a single geometric set of a mutual inductance values with $10 \ldots 20$ elements with a turns discretization (i.e., values of a K and N) of the order 2^{10}. Thus, performance evaluation of a single design version with three uncontrolled geometric parameters (distance, shift, inclination) can take about $1 \ldots 10$ hours depending on the problem discretization. This time should be multiplied by the number of design versions studied during the optimization procedure.

All in all, it can be said that we achieved reasonably short calculation time and obtained significant time gain as opposed to the host CPU computing. We compared calculation time using the proposed GPU computing method, sequential calculation (loop "for" in MATLAB) on the host CPU (Intel Xeon X5660, 2.8 GHz) and parallel calculation (loop "parfor" in MATLAB) on the host CPU (6 kernel, 12 parallel threads for the CPU) for a single geometric set of mutual inductance values (10 elements). It was found that the calculations using our method were about $50 \ldots 80$ faster than sequential calculation on the host CPU and about $5 \ldots 10$ in comparison with parallel computing on the host CPU with the turns discretization of the order 2^{10}.

In order to evaluate the significance of the assumption of the inclination angle smallness mentioned in the beginning of Section 2, we have compared results obtained with the help of Equations (2) and (4) (see Fig. 3). Geometry was set as typical for biomedical application, with axial distance less than coils external radii (20 and 35 mm, respectively) and significant lateral displacement (30 mm). It was found for the chosen geometry that mutual inductance calculation relative error is less than 3%, if the inclination angle does not exceed 20 degrees. By contrast, calculation time using exact Equation (2) is about 1.3 times higher than the calculation time using approximate Equation (4). Thus, Equation (4) can be considered more suitable for practical application of the proposed method in the case of relatively small angular displacements.

3.2. Comparison with Electromagnetic Field Solvers

Unlike computing using CPU, computing using electromagnetic field solvers (EFS) cannot be compared with the proposed method directly. There are no variables analogous to the geometric parameter discretization or turns discretization of the proposed algorithm. Another thing to consider, when we evaluate the computation time using EFS, is the space dimension in which we solve our problem. The simple case of the mutual inductance calculation of two perfectly aligned coaxial coils can be solved in two-dimensional axisymmetrical space (2D). However, when either inclination or lateral misalignment of the coils is added, the problem must be solved in three-dimensional space (3D). Therefore, the complexity of the problem and computation time rise significantly.

Nevertheless, it is possible to validate accuracy of our method with EFS, COMSOL Multiphysics

(a)   (b)
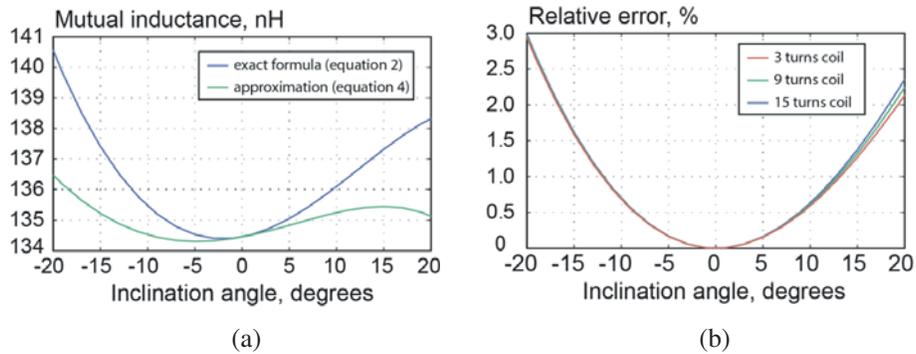
Figure 3. (a) Mutual inductance as a function of the inclination angle (a) for spiral planar coils obtained via exact Equation (2) (solid line) and approximate Equation (4) (dotted line). Number of turns in both coils is 3, the external coil radii are 35 mm, axial distance between the coils is 20 mm, lateral distance is 30 mm). (b) Relative error of mutual inductance calculation for the same geometry and coils with 3 (solid line), 9 (dashed line) and 15 (dotted line) turns in each.
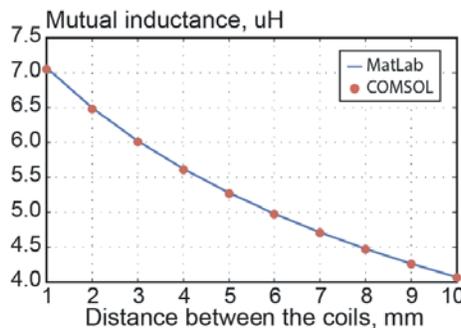
Figure 4. The mutual inductance between the transmitting and receiving coil as a function of an axial distance of the two spiral coils calculated using proposed method (solid line) and COMSOL field solver (dashed line). Geometrical parameters of the coils are as following: outer radii of the coils 70 mm, each coil consists of 5 turns, the distance between the turns is 1.2 mm. Discretization of the turns for the proposed method is 2^{10}.

for instance. We solved 2D case of the two perfectly aligned coils using EFS with 1% accuracy. Chosen outer radii of the coils was 70 mm. Each coil consists of 5 turns, and the distance between the turns is 1.2 mm. Solution for the same parameters with the same accuracy was calculated using our method and compared with the EFS results. Discretization of the turns is set to 2^{10}. Results for this example are depicted in Fig. 4.

First of all, it should be noted that we achieved accuracy comparable to the accuracy of EFS (Fig. 4). Computation time in COMSOL was about 17 seconds, and computation time using GPU was about 3 seconds. In general, time gain in comparison to cases which can be described in EFS using 2D geometry is about 5 ... 7. More importantly, as our tool is suitable for evaluation of the complex geometry, the greatest time gain results from the fact that calculation time in our method did not depend on values of fixed uncontrolled parameters, whether they are equal to zero or not. It is not the case for EFS, as mentioned above. Thus, if we evaluate the mutual inductance of the two misaligned coils, we can achieve time gain of the order from 100 and higher.

3.3. Experimental Verification

The results of the modeling were verified by the measurements. Equivalent circuit of the experimental rig is given in Fig. 5. Transmitting and receiving coils are connected to the corresponding printed circuit boards (PCBs) via terminal blocks, thus are easily switchable in order to be able to test different
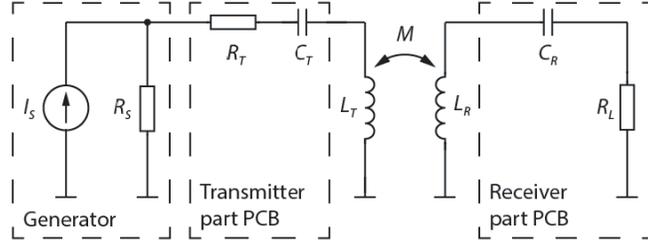
Figure 5. Schematic representation of the experimental rig. Transmitter and receiver parts PCBs provide series compensation of the corresponding inductances.

coils geometries. In the experiment, the transmitter coil configuration matched with the receiver coil configuration. Radii of the coils used in experimental measurements were 104 mm. Number of turns was 3, and wire cross-section radius was 0.4 mm. Transmitting and receiving coils were perfectly aligned during the experiment. Effect of the distance between the coils centers on the mutual inductance was investigated.

The generator block includes function generator (Tektronix AFG3252) that produces ideal sinusoidal signal and provides convenient regulation of the operating frequency. Frequency range of the generator is from 10 kHz to 230 MHz, hence fully covers frequencies of interest in researches of the TET. Transmitter part PCB includes test resistor and compensating circuit (series, parallel or series-parallel) for the primary inductance L_T. For the described experiment series compensation was chosen. Similarly, receiver part PCB includes load resistor and compensating circuit for the secondary inductance L_R. Resistance of the receiving part is not used explicitly as a distinct component in the presented figure. However, it can be thought as a part of the load resistance and does not qualitatively affect the conclusions provided further. For the secondary part series compensation was also chosen. The circuit parameters used for the described experiment are given in Table 1.

Table 1. Parameters of the experimental rig used in the experiment.

Parameter	Value	Description
I_S	0.071 A	Output current of the generator
R_S	50 Ohm	Internal resistance of the generator
R_T	20 Ohm	Resistance of the transmitting part of the system
R_L	20 Ohm	Load resistance
C_T	1.5 nF	Capacitance of the transmitting part oscillator
C_R	1.5 nF	Capacitance of the receiving part oscillator

Figure 6 shows measured and calculated mutual inductances dependent on distance between the coils. As we can see, the measured results closely follow the curve calculated by the tool presented in Section 2 despite the simplifications assumed in the method.

As will be shown later, mutual inductance by itself is not a well suited metric for the IPU optimization. It is more instructive to compute IPU output characteristics (i.e., load power, load voltage, energy transfer efficiency) using results of a mutual inductance calculation. In this paper, the load power is used as a main IPU metric. For given series-primary series-secondary compensated topology shown in Fig. 5, the load power can be calculated using KVL. Resulting equation for the output power of the system is:

$$P_L = \frac{\omega^2 M^2 I_S^2 R_S^2 R_L}{(Z_T Z_R + Z_R R_S + \omega^2 M^2)^2},$$
(13)

here, Z_T is impedance of the transmitter, Z_R the impedance of the receiver, and the corresponding
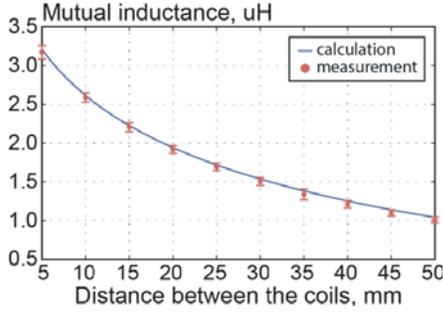
Figure 6. Calculated (solid line) and measured (dots) values of the mutual inductance between the transmitting and receiving coil as a function of the axial distance between the coils. Radii of the coils is 104 mm, number of turns is 3, wire cross-section radius is 0.4 mm. Results of the measurements are in good agreement with the curve calculated by the tool presented in Section 2.
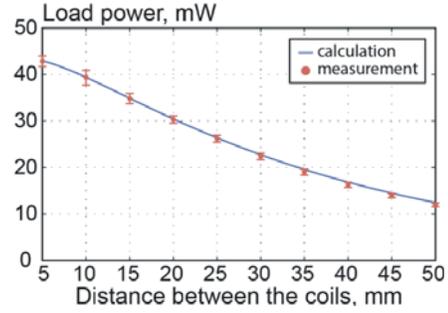
Figure 7. Calculated (solid line) and measured (dots) values of the transferred power (b) as a function of an axial distance. IPU parameters are given in Table 1. Results of the measurements are in good agreement with the curve calculated by the tool presented in Section 2.

formulas for calculation of the impedances are:

$$Z_T = R_T + j\omega L_T + \frac{1}{j\omega C_T}, \tag{14}$$

$$Z_R = R_L + j\omega L_R + \frac{1}{j\omega C_R}. \tag{15}$$

Figure 7 shows the load power as a function of distance between the coils. It can be seen that results of calculation are well within error bound.

4. EXEMPLARY DESIGN PROCEDURE: RANGE CIRCUIT OPTIMIZATION

In this section, exemplary procedure is given for an IPU optimization using the proposed method. Changing geometric conditions is one of the main features of the IMD inductive powering. It means that designers should optimize IPU for a range of uncontrolled parameters by the adjustment of controlled ones.

Our method can be applied to a design optimization in the following manner:

1. Define the design requirements and design constants. Requirements for the range of the output power, operating frequency range, all of the controlled and uncontrolled geometric parameters must be set.

2. Calculate mutual inductance for a given range of uncontrolled parameters and given values of controlled parameters (i.e., design version).

3. Calculate IPU performance metrics on the basis of a mutual inductance calculation.

4. Compare design requirements with calculation results.

5. If design goals are not achieved, iterate procedure for another design version.

Tuning of the chosen controlled parameters is the core of the optimization process. Higher number of parameters involved into the tuning can lead to improved results of an IPU operation in terms of size and efficiency. However, this number is commonly restricted by the application specific itself (most often, limitations apply to the outer radius of the coils) and not only by the designer's decision. At the same time, the number of parameters being adjusted essentially defines the complexity of the procedure.

In our example, we adjust the number of turns of the cylindrical coils to obtain desired output power for the defined range of axial distance between the coils. Other uncontrolled parameters are

assumed constant to clarify the optimization procedure description. Also, for the better clarity of the results presentation, the case of the single parameter tuning is considered in our example: only number of turns for the both coils is adjusted to achieve required output power in the defined range of the coils misalignments. Parameters of the system are equal to the ones given in Table 1. Main design requirements are output power in range 40 ... 45 mW for the axial distance between the coils from 20 to 35 mm. Outer radii of the coils are 100 mm.

Results of the mutual inductance calculation are shown in Fig. 8(a). It can be seen that there are monotonic dependencies for both the uncontrolled parameter (the mutual inductance decreases with the rising distance between the coils) and controlled one (the mutual inductance increases with the turns number increase). Thus, the optimization cannot be performed using mutual inductance as an only performance metric. Geometric evaluation of a load power gives more interesting picture (Fig. 8(b)). We can observe curves with local maximum, which is desired situation for the optimization procedure. Fig. 8(b) depicts that the seven-turn coil is the most suited geometrical configuration for the given design requirements (the results of the calculations are illustrated for the number of turns of the coils from 4 to 8. The results obtained for the lesser number of turns are not shown due to the low output power). Modeling results were verified with experimental rig using inductive link designed on the basis of the calculations (Fig. 9).

The procedure described above can serve as a basis for the real IPU design. The optimization

(a)　　　　　　　　　　　　(b)
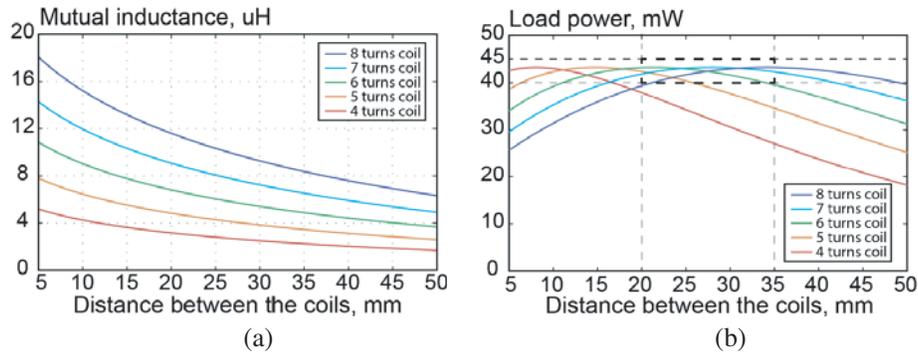
Figure 8. (a) Mutual inductance between the transmitting and receiving coils and (b) load power as a function of the distance between the coils for the various number of turns: 4 turns (red), 5 turns (orange), 6 turns (green), 7 turns (cyan), 8 turns (blue). Grid lines show range of the output power and the distance between the coils defined by the application. Increase in number of turns between the coils lead to increase in mutual inductance. However, situation with load power is less self-evident. Increase in number of turns moves peak power between the coils farther away from initial point. It can be seen that the coil with 7 turns is appropriate solution for the given design constraints.
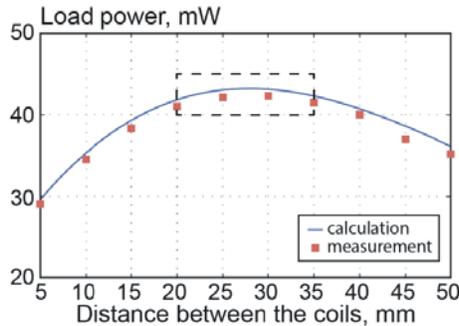
Figure 9. Load power as a function of the distance between the coils. Results calculated by Equation (13) (blue line) are verified by the measured data (red squares). Bold grid square shows range of interest for output power and the distance between the coils defined by the application.

procedure returns set of the most suited controlled parameters for the given range of uncontrolled parameters of an inductive link. It is worth noting that in real IPU application every type of coils misalignment must be considered. Therefore, design procedure will be more difficult than the one described above. However, in many cases additional controlled parameters will be at designer's disposal (e.g., outer coil radii and distance between the coil turns), thus providing additional capabilities for optimization.

5. CONCLUSION

We have described the method for geometric evaluation of a mutual inductance using parallel computing on GPU. It was developed as a result of our activity in the design of an inductive powering unit for implanted medical device. In the course of our work we found that despite providing high accuracy and being powerful tool for other tasks, existing electromagnetic field solvers are not well suited for geometric evaluation of a mutual inductance due to long computation times in case of misalignments and specific geometries. Geometry plays key role in an IPU design and appropriate means for a fast and accurate study of a geometric influence on IPU characteristics is badly needed. It was shown that such means can be developed on the basis of a GPU computing and MATLAB coding.

We achieved significant time gain in comparison with the host CPU computing using MATLAB (up to 80 for sequential summation and up to 8 for a parallel computing). We should note once more that our method can be easily implemented by designers and engineers with only basic knowledge in GPU computing algorithm due to its relative simplicity. Even better results in terms of computation speed can be achieved with more sophisticated code that utilizes optimized CPU + GPU architecture.

Precision of the developed method was compared with the precision of the EFS. We found that the precision of our method was comparable to the EFS precision, and at the same time, computation time was substantially less (time gain is about 7 . . . 8 for 2D case and about 100 and higher for 3D case). Also we have experimentally verified our method and shown that results of the calculations are accurate enough to predict real IPU performance. At the same time, we purposely simplified the mathematics that our method is based on to achieve additional time gain and maximal speeding up of the computations (i.e., simplest form of the Neumann's formula (i.e., expression for infinitely thin filaments) and the simplest way of a numerical integration (i.e., rectangle method) were used).

The developed method was used for the analysis of an IPU performance in changing geometric circumstances in order to optimize an inductive link. In our example, we found optimal value of a controlled parameter (i.e., number of a coils turns) which provide stable output characteristics (i.e., load power) in a given range of geometric parameter (i.e., axial distance).

Our general goal was to provide the possibility of a thorough analysis of an IPU geometry in a reasonably short time. The described method can be used for a study of an IMD inductive powering as a general phenomenon as well as for a proper design of a particular IPU for biomedical applications.

At the same time, these are not the only possible applications for our results. They can be used for development of the CAD system aimed at biomedical IPU. Also, there is a noticeable interest in a coils positioning method for an IPU performance improvement [22, 24]. Precalculated mutual inductance matrices are used in such methods. Our method provides possibility for almost real-time calculation of mutual inductance values for at least one uncontrolled geometric parameter. Thus, if there is wireless link between IMD and host station with GPU unit, parallel computing of a mutual inductance can be used in coils positioning algorithms, and it allows to additionally increase accuracy in comparison with methods using precalculated matrices

REFERENCES

1. Bocan, K. and E. Sejdic, "Adaptive transcutaneous power transfer to implantable devices: A state of the art review," *Sensors*, Vol. 16, No. 3, 393, 2016.

2. Lenaerts, B. and R. Puers, *Omnidirectional Inductive Powering for Biomedical Implants*, Springer, Netherlands, 2009.

3. Yakovlev, A., S. Kim, and A. Poon, "Implantable biomedical devices: Wireless powering and communication," *IEEE Commun. Mag.*, Vol. 50, No. 4, 152–159, 2012.

4. Zeng, F.-G., S. Rebscher, W. Harrison, X. Sun, and H. Feng, "Cochlear implants: System design, integration and evaluation," *IEEE Rev. Biomed. Eng.*, Vol. 1, 115–142, 2008.

5. Bradley, K., "The technology: The anatomy of a spinal cord and nerve root stimulator: The lead and the power source," *Pain Med.*, Vol. 7, No. SUPPL 1, S27–S34, 2006.

6. Zhou, D. and E. Greenbaum, *Implantable Neural Prostheses 1. Devices and Applications*, Springer-Verlag, New York, 2009.

7. Weiland, J., W. Liu, and M. Humayun, "Retinal prosthesis," *Annu. Rev. Biomed. Eng.*, Vol. 7, 361–401, 2005.

8. Li, X., Y. Yang, and Y. Gao, "Visual prosthesis wireless energy transfer system optimal modeling," *Biomed. Eng. Online*, Vol. 13, No. 1, 2014.

9. Baumgart, R., P. Thaller, S. Hinterwimmer, M. Krammer, T. Hierl, and W. Mutschler, "A fully implantable, programmable distraction nail (fitbone) — New perspectives for corrective and reconstructive limb surgery in practice of intramedullary locked nails," *Practice of Intramedullary Locked Nails*, 189–198, Springer, Berlin, Heidelberg, 2006.

10. Bergmann, G., F. Graichen, J. Dymke, A. Rohlmann, G. N. Duda, and P. Damm, "High-tech hip implant for wireless temperature measurements in vivo," *PLoS One*, Vol. 7, No. 8, e43489, 2012.

11. Wang, J., J. Smith, and P. Bonde, "Energy transmission and power sources for mechanical circulatory support devices to achieve total implantability," *Ann. Thorac. Surg.*, Vol. 97, No. 4, 1467–1474, 2014.

12. Slaughter, M. and T. Myers, "Transcutaneous energy transmission for mechanical circulatory support systems: history, current status, and future prospects," *J. Cardiac Surg.*, Vol. 25, No. 4, 484–489, 2010.

13. Danilov, A. A., G. P. Itkin, and S. V. Selishchev, "Progress in methods for transcutaneous wireless energy supply to implanted ventricular assist devices," *Biomed. Eng.*, Vol. 44, No. 4, 125–129, 2010.

14. Puers, R. and G. Vandervoorde, "Recent progress on transcutaneous energy transfer for total artificial heart System," *Artif. Organs*, Vol. 25, No. 5, 400–405, 2001.

15. Leung, H. Y., D. M. Budgett, and A. P. Hu, "Minimizing power loss in air-cored coils for TET heart pump systems," *IEEE J. Emerg. Sel. Top. Circuits Syst.*, Vol. 1, No. 8, 412–419, 2011.

16. Choi, S.-W. and M.-H. Lee, "Coil-capacitor circuit design of a transcutaneous energy transmission system to deliver stable electric power," *ETRI J.*, Vol. 30, No. 6, 844–849, 2008.

17. Bock, D., A. Marschilok, K. Takeuchi, and E. Takeuchi, "Batteries used to power implantable biomedical devices," *Electrochim. Acta*, Vol. 84, 155–164, 2012.

18. Amar, A., A. Kouki, and H. Cao, "Power approaches for implantable medical devices," *Sensors*, Vol. 15, No. 11, 28889–28914, 2015.

19. Larsson, B., H. Elmqvist, L. Ryden, and H. Shueller, "Lessons from the first patient with an implanted pacemaker: 1958–2001," *PACE*, Vol. 26, No. 1, Pt. 1, 114–124, 2003.

20. Schuder, J. C., "Powering an artificial heart: Birth of the inductively coupled-radio frequency system in 1960," *Artif. Organs*, Vol. 26, No. 11, 909–915, 2002.

21. Jegadeesan, R. and Y.-X. Guo, "Topology selection and efficiency improvement of inductive power links," *IEEE T. Antenn. Propag.*, Vol. 60, No. 10, 4846–4854, 2012.

22. Hu, L., Y. Fu, X. Ruan, H. Xie, and X. Fu, "Detecting malposition of coil couple for transcutaneous energy transmission," *ASAIO J.*, Vol. 62, No. 1, 56–62, 2016.

23. Danilov, A. A. and E. A. Mindubaev, "Influence of angular coil displacements on effectiveness of wireless transcutaneous inductive energy transmission," *Biomed. Eng.*, Vol. 49, No. 3, 171–173, 2015.

24. Friedmann, J., F. Groedl, and R. Kennel, "A novel universal control scheme for transcutaneous energy transfer (TET) applications," *IEEE J. Emerg. Sel. Top. Circuits Syst.*, Vol. 3, No. 1, 296–

305, 2015.

25. Ghovanloo, M., "An overview of the recent wideband transcutaneous wireless communication techniques," *33rd Annual International Conference of the IEEE EMBS*, 5864–5867, 2011.

26. Zierhofer, C. M. and E. S. Hochmair, "Geometric approach for coupling enhancement of magnetically coupled coils," *IEEE Trans. Biomed. Eng.*, Vol. 43, No. 7, 708–714, 1996.

27. Jow, U.-M. and M. Ghovanloo, "Design and optimization of printed spiral coils for efficient transcutaneous inductive power transmission," *IEEE Transactions on Biomedical Circuits and Systems*, Vol. 1, No. 3, 193–202, 2007.

28. Danilov, A. A., E. A. Mindubaev, and S. V. Selishchev, "Space-frequency approach to design of displacement tolerant transcutaneous energy transfer system," *Progress In Electromagnetics Research M*, Vol. 44, 91–100, 2015.

29. Babic, S. and C. Akyel, "New formulas for mutual inductance and axial magnetic force between magnetically coupled coils: Thick circular coil of the rectangular cross-section-thin disk coil (pancake)," *IEEE T. Magn.*, Vol. 49, No. 7, 860–868, 2013.

30. Babic, S., F. Sirois, C. Akyel, G. Lemarquand, V. Lemarquand, and R. Ravaud, "New formulas for mutual inductance and axial magnetic force between a thin wall solenoid and a thick circular coil of rectangular cross-section," *IEEE T. Magn.*, Vol. 47, No. 8, 2034–2044, 2011.

31. Babic, S. I. and C. Akyel, "Calculating mutual inductance between circular coils with inclined axes in air," *IEEE T. Magn.*, Vol. 44, No. 7, 1743–1750, 2008.

32. Conway, J. T., "Inductance calculations for noncoaxial coils using Bessel functions," *IEEE T. Magn.*, Vol. 43, No. 3, 1023–1034, 2007.

33. Conway, J. T., "Noncoaxial inductance calculations without the vector potential for axisymmetric coils and planar coils," *IEEE T. Magn.*, Vol. 44, No. 4, 453–462, 2008.

34. Conway, J. T., "Exact solutions for the mutual inductance of circular coils and elliptic coils," *IEEE T. Magn.*, Vol. 48, No. 1, 81–94, 2012.

35. Conway, J. T., "Analytical solutions for the self and mutual inductances of concentric coplanar disk coils," *IEEE T. Magn.*, Vol. 49, No. 3, 1135–1142, 2013.

36. Babic, S. and C. Akyel, "Magnetic force between inclined circular filaments placed in any desired position," *IEEE T. Magn.*, Vol. 48, No. 1, 69–80, 2012.

37. Babic, S., F. Sirois, C. Akyel, and C. Girardi, "Mutual inductance calculation between circular filaments arbitrarily positioned in space: Alternative to Grover's formula," *IEEE T. Magn.*, Vol. 46, No. 9, 3591–3600, 2010.

38. Soma, M., D. C. Galbraith, and L. W. White, "Radio-frequency coils in implantable devices: Misalignment analysis and design procedure," *IEEE Trans. Biomed. Eng.*, Vol. BME-34, No. 4, 276–282, 1987.

39. Kalantarov, P. L., *Inductance Calculations*, National Power Press, Moscow, 1955.

40. Krasteva, V. T., S. P. Papazov, and I. K. Daskalov, "Magnetic stimulation for non-homogeneous biological structure," *Biomed. Eng. Online*, Vol. 1, 2002.

41. Ahma, L., M. Ibrani, and E. Hamiti, "Computation of SAR distribution in a human exposed to mobile phone electromagnetic fields," *PIERS Proceedings*, 1580–1582, Xi'an, China, March 22–26, 2010.

42. Ke, L., G. Yan, S. Yan, Z. Wang, and D. Liu, "Improvement of the coupling factor of Litz-wire coil pair with ferrite substrate for transcutaneous energy transfer system," *Progress In Electromagnetics Research M*, Vol. 39, 41–52, 2014.

43. Owens, J. D., M. Houston, D. Luebke, S. Green, J. E. Stone, and J. C. Phillips, "GPU computing," *P. IEEE*, Vol. 96, No. 5, 879–889, 2008.

44. Nickolls, J. and W. J. Dally, "The GPU computing era," *IEEE Micro.*, Vol. 30, No. 2, 56–69, 2010.